AGU PUBLICATIONS

JGR

Journal of Geophysical Research: Space Physics

RESEARCH ARTICLE
10.1002/2015JA021809

Key Points:
- The IMF B_x component is converted into opposite polarities of the magnetosheath B_z in different hemispheres
- The B_z near the magnetopause changes over time under the radial IMF conditions
- The asymmetric reconnection affects the magnetic fields of the magnetosheath and magnetosphere

Correspondence to:
J.-H. Shue,
jhshue@jupiter.ss.ncu.edu.tw

Citation:
Pi, G., J.-H. Shue, K. Grygorov, H.-M. Li, Z. Němeček, J. Šafránková, Y.-H. Yang, and K. Wang (2017), Evolution of the magnetic field structure outside the magnetopause under radial IMF conditions, *J. Geophys. Res. Space Physics*, *122*, 4051–4063, doi:10.1002/2015JA021809.

Received 14 AUG 2015
Accepted 15 MAR 2017
Accepted article online 20 MAR 2017
Published online 4 APR 2017

Evolution of the magnetic field structure outside the magnetopause under radial IMF conditions

Gilbert Pi[1,2], Jih-Hong Shue[1], Kostiantyn Grygorov[2], Hsien-Ming Li[1], Zdeněk Němeček[2], Jana Šafránková[2], Ya-Hui Yang[1], and Kaiti Wang[3]

[1]Institute of Space Science, National Central University, Taoyuan, Taiwan, [2]Faculty of Mathematics and Physics, Charles University, Prague, Czech Republic, [3]Department of Aerospace Engineering, Tamkang University, New Taipei City, Taiwan

Abstract We use the Time History of Events and Macroscale Interactions during Substorms data to investigate the magnetic field structure just outside the magnetopause and its time evolution for radial interplanetary magnetic field (IMF) events. When the magnetic field drapes around the magnetopause in the magnetosheath region, an asymmetric magnetic field orientation in different hemispheres is expected. Our two-case study reveals some conflicts with the predicted draped field configuration in the Southern Hemisphere. The magnetosheath B_z component had a different sign depending on the upstream IMF B_x component's polarity at the beginning of the radial IMF intervals. With time, the observed B_z became northward in both cases with increasing positive values through the events. The increasing value of the B_z component may be explained by two possible mechanisms: by a change of the upstream IMF and by a reconnection between magnetosheath and magnetospheric field lines. Our study shows that both mechanisms contributed to the observed changes. Thus, there was a correlation between the change of the upstream IMF conditions and an increase in the magnetosheath northward magnetic field component. The observed formation of the boundary layer near the magnetopause proves that the reconnection process was ongoing at least for a part of the time. We suggest two possible reconnection scenarios: one near subsolar point and another tailward of the one cusp due to lobe reconnection. The asymmetry of reconnection locations causes rearrangement of the magnetic field structure near the magnetopause and turns the observed magnetosheath B_z component even further into positive values.

1. Introduction

The long-duration radial interplanetary magnetic field (IMF) events are unique phenomena in the interplanetary space. The magnetic field of the Sun propagates with the solar wind because of the frozen-in condition. Considering the solar rotation and solar wind speed around 400 km/s, IMF evolves into spiral geometry [*Parker*, 1958]. The angle between IMF and the Sun-Earth line approaches 45° near the Earth orbit under average solar wind conditions. Although the local disturbances or transient solar eruptions, such as during a coronal mass ejection, may change the orientation of the IMF, the IMF cannot be maintained in the radial direction for a long period (more than 6 h). The radial IMF events are often found in the trailing region of high-speed streams [*Neugebauer et al*., 1997; *Jones et al*., 1998; *Watari et al*., 2005]. On average, typical values of all solar wind parameters for the radial IMF are lower and quieter than those for other IMF orientations [*Neugebauer et al*., 1997; *Watari et al*., 2005; *Pi et al*., 2014]. The solar wind speed, the strength of the IMF, ion density, and ion temperature are reduced by 7%, 18%, 22%, and 36%, respectively [*Pi et al*., 2014]. Nevertheless, when the radial IMF approaches the bow shock, it can lead to a disturbed magnetosheath and distorted magnetopause shape.

The radial IMF can lead to some changes in the magnetospheric system. First, the foreshock region moves to the front side near the subsolar nose of the bow shock, creating foreshock bubbles [*Omidi et al*., 2010]. Second, the total pressure in the magnetosheath is much lower than the upstream solar wind dynamic pressure [*Samsonov et al*., 2012]. Behind the quasi-parallel bow shock, the magnetosheath is more turbulent than that downstream of the quasi-perpendicular shock. The supersonic earthward jets [*Sundkvist et al*., 2007; *Hietala et al*., 2009] and the high-speed sunward plasma jets [*Shue et al*., 2009] can be found in the magnetosheath. The thickness of the magnetosheath also decreases in response to the radial IMF conditions as a result of expanded magnetopause [*Jelínek et al*., 2010]. The previous results show that the magnetopause moves about 2 R_E sunward in comparison with the model predictions, having a bullet-like or globally expanded structure [*Slavin et al*., 1996; *Dušík et al*., 2010; *Jelínek et al*., 2010; *Suvorova et al*., 2010, *Suvorova*

and Dmitriev, 2015a, 2015b, *Park et al*., 2016]. The magnetopause also shows a local time asymmetry in its size and shape [*Huang et al*., 2015]. It was reported that empirical models underestimate the magnetopause position in the postnoon sector (12–17 magnetic local time (MLT)) and overestimate the magnetopause positions in the dawn (5–8 MLT) and dusk (18–21 MLT) sectors. These results may be related to the pressure variations created in the foreshock region, and these variations can lead to an additional oscillation of the magnetopause [*Russell et al*., 1997]. *Pi et al*. [2016] carried out a case study showing that IMF B_x turns into B_y and B_z in the magnetosheath as it drapes around the magnetopause. *Tang et al*. [2013] investigated the magnetospheric structure under radial IMF conditions using the global magnetohydrodynamic simulations. The draped field is also seen in their results. Similarly, *Petrinec* [2016] reported the draped field occurring rather far downstream of the bow shock under the radial IMF conditions.

Dayside reconnection is one of the major mechanisms that govern the global magnetic field structure near the magnetopause. During the southward IMF, reconnection most likely occurs near the subsolar point at the magnetopause [*Dungey*, 1961] and creates two open field lines. The new open field lines will move tailward with the solar wind flow and transfer the magnetic flux to flanks of the magnetotail. During the northward IMF, reconnection most likely occurs in the region behind the cusp [*Dungey*, 1963; *Crooker*, 1979; *Song and Russell*, 1992; *Song et al*., 1999]. Reconnection can happen in one hemisphere, a single lobe reconnection, or in both hemispheres, dual lobe reconnection. Single lobe reconnection creates open field lines connecting the magnetic field in the magnetosheath and the magnetosphere. Dual lobe reconnection only happens under a strong northward IMF, and it creates new reclosed field lines [e.g., *Bogdanova et al*., 2013]. Under the radial IMF conditions, the draping effect forms an asymmetry of the field orientation in the magnetosheath: the orientations of the B_z component are opposite in the different hemispheres. Therefore, reconnection location would be asymmetric in different hemispheres, which is supported by the simulation results by *Tang et al*. [2013].

In this paper, we used the Time History of Events and Macroscale Interactions during Substorms (THEMIS) data to show the magnetic field structure just outside the magnetopause and its evolution over time for two long-duration events with the radial IMF. The first section includes a brief introduction to this study, and section 2 describes the data we used. Section 3 shows the results of the THEMIS observations, and section 4 contains the discussion and interpretation. The conclusions are presented in section 5.

2. Data

The THEMIS mission [*Sibeck and Angelopoulos*, 2008] is composed of five probes. Due to their low inclination orbits, THEMIS mission provides frequent dayside magnetopause crossings near the equatorial plane. In this study, we use the data from the electrostatic analyzer [*McFadden et al*., 2008] and the fluxgate magnetometer [*Auster et al*., 2008] on board the THEMIS probes to investigate the magnetic field in the magnetosheath and its evolution. The 5 min resolution OMNI data [*King and Papitashvili*, 2005] are used to infer corresponding solar wind conditions.

We used a definition of the long-duration ($>$4 h) radial IMF events proposed by *Pi et al*. [2014]. These events were selected from the OMNI data using a criterion of $|B_x|/B \geq 0.9$, where B is the IMF magnitude and B_x is the X component of the IMF in the GSM coordinates. The persisting time interval should be longer than 4 h. In total, 52 long-duration events were recorded during the period from 2007 to 2011. One of our major goals is to understand how the magnetic field drapes around the magnetopause. Thus, we used these radial IMF events and the corresponding magnetopause crossings compiled by *Shue et al*. [2011] in the event search process. We skipped the magnetopause crossing during the first hour of the radial IMF period. Therefore, the corresponding solar wind conditions can easily be obtained without needing to consider the error of propagation time. Finally, we found two events with multiple magnetopause crossings. This kind of events is suitable to study the evolution of the magnetic field in the magnetosheath, especially near the magnetopause.

3. Results

We analyzed two events with the opposite IMF B_x polarities during the intervals of radial IMF when the whole dayside magnetopause is behind the quasi-parallel bow shock. The first case, with the duration of about 4 h, occurred on 12 July 2007. During the period, all the THEMIS probes were orbiting in the Southern Hemisphere

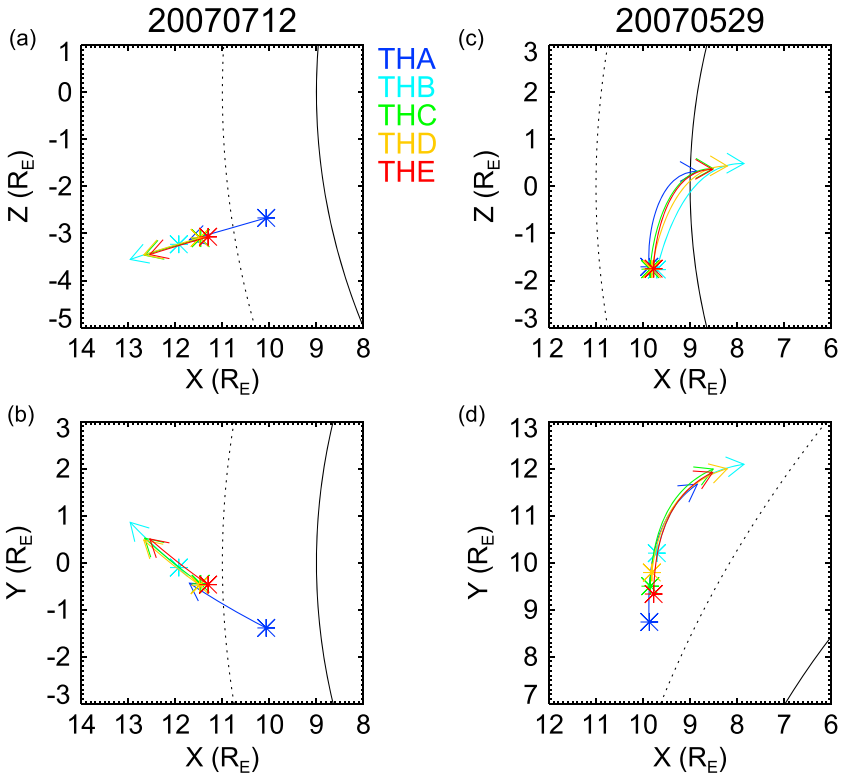

Figure 1. The trajectories of the THEMIS probes in the GSM coordinate on 12–13 July 2007 and 29 May 2007. The different colors denote the different THEMIS probes, and the arrows show the moving direction along the trajectories of the probes from 2200 UT on 12 July to 0200 UT on 13 July and 1700 to 2300 UT on 29 May. The trajectories are plotted (a, c) in the *XZ* plane and (b, d) in the *XY* plane. The dotted and black lines in each panel represent the bow shock and magnetopause locations, respectively.

and close to the Sun-Earth line (Figures 1a and 1b, drawn in the GSM coordinates). The THEMIS probes did not have a large separation (2 R_E in the *X* direction, 1 R_E in the *Y* direction, and 0.5 R_E in the *Z* direction) and had almost the same trajectories. The other case occurred on 29 May 2007, with the radial IMF persisting for about 5 h. The THEMIS probes were moving toward the dayside magnetosphere at 15 MLT in this case, but they were located close to the *XY* plane (Figures 1c and 1d). Due to a longer duration of this event than our first case, the displacements of the THEMIS probes are noticeable. The probes moved from 8 to 12 R_E in the *Y* direction. Nevertheless, both cases can be used for a study of the north-south asymmetry of the magnetosheath magnetic field configuration for radial IMF. In Figure 1, the two black lines show the positions of the magnetopause (solid) and the bow shock (dotted) calculated from the models of *Shue et al.* [1997] and *Chao et al.* [2002], respectively. The probes orbited in a considerably large distance outside the modeled magnetopause, but numerous magnetopause crossings were recorded during the two events. The discrepancy indicates that the model underestimates the magnetopause locations.

Figure 2 shows the data in the GSM coordinates from THEMIS B for the 12 July 2007 event. Figures 2a–2d show the temporal variations of the magnetic field vector, plasma speed, proton density, and temperature, respectively, observed by THEMIS B, and Figures 2e–2g show the corresponding IMF vector, the V_y and V_z components of the solar wind velocity, and density from the OMNI database. It can be seen that the magnetic field changed, especially its B_z component, in the magnetosheath although the upstream IMF is stable. The magnetosheath B_z was small and fluctuating between 2232 and 2236 UT. THEMIS B entered the magnetosheath again at 2304 UT and observed gradually increasing magnetosheath B_z to +20 nT prior to a short visit of the magnetosphere. After that, THEMIS B observed the positive magnetosheath B_z until 0000 UT. Between 0000 and 0015 UT, magnetosheath B_z became small with short periods of negative values. The last THEMIS B magnetosheath interval (0105–0135 UT) is characterized by the fluctuating B_z component with large negative excursions at the end of the interval. For all three THEMIS B

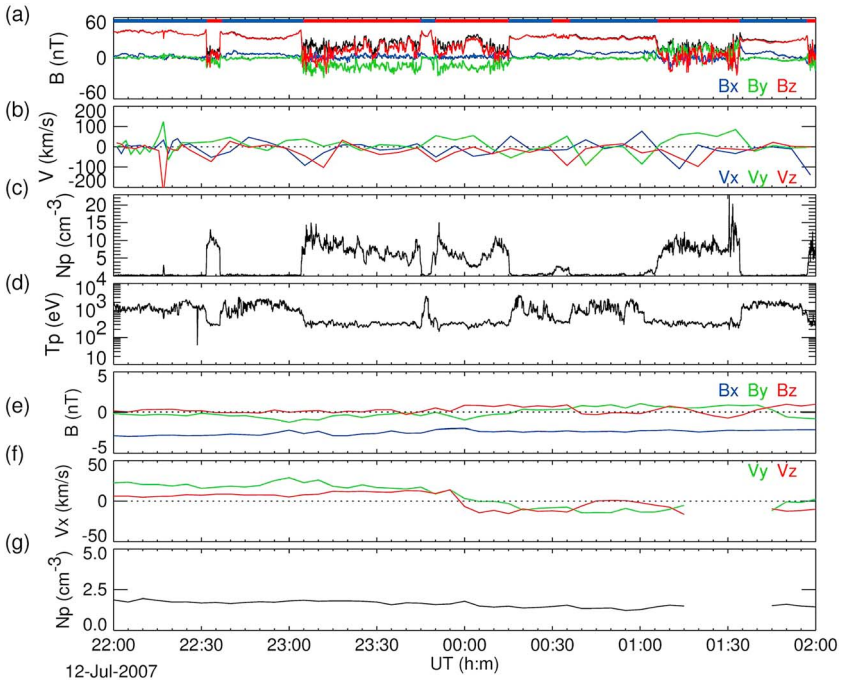

Figure 2. The magnetic field and plasma data changes over time on 12–13 July 2007. The three components of the (a) magnetic field, (b) plasma speed in the GSM coordinate, (c) proton number density, and (d) proton temperature are arranged. These parameters were obtained from THEMIS B. The simultaneous observations of the (e) magnetic field, (f) solar wind speed, and (g) proton density from the OMNI database. The horizontal bars that denote the probe location is in the magnetosheath (red) and in the magnetosphere (blue).

magnetosheath intervals (2232–2236 UT, 2304–0015 UT, and 0101–0135 UT), the magnetosheath B_x was very small but it exhibited notable fluctuations in the last interval. In the first interval, B_y was around zero and became negative in the second interval. In the last interval, THEMIS B also observed fluctuating B_y but with a positive mean value.

THEMIS B was mainly in the magnetosphere, visiting the magnetosheath only for limited periods, but its magnetosheath observations can be complemented with other THEMIS probes that provided similar observations due to their similar trajectories. To clearly show the trend of the magnetosheath magnetic field variations, we plot each magnetic field component just outside the magnetopause from all the THEMIS probes in Figure 3. Numerous magnetopause crossings were recorded from 2220 UT on 12 July to 0140 UT on 13 July 2007. We identified the periods when the probes were located in the magnetosheath. If such a period was shorter than 5 min, we took the average of each component of the magnetic field during this period; otherwise, we took the average for the first 5 min adjacent to the magnetopause at the magnetosheath side. As it is shown in Figure 3, these averages are marked by crosses, and the error bars show the standard deviations of the data. Figure 3a shows the B_x variation in the region adjacent to the magnetopause. The magnitude of B_x was always small showing the maximum value of about 5 nT during this event. The B_y component was negative, and its value was fluctuating from -5 to -25 nT at the beginning of the event (Figure 3b), but it turned to positive values after 0030 UT. The B_z component started with a value around zero and became increasingly positive from 2200 UT on 12 July to 0000 UT on 13 July (Figure 3c). There was no spacecraft in the magnetosheath until 0100 UT, and observations show that B_z was southward when the spacecraft entered the magnetosheath after 0100 UT.

The data recorded by THEMIS B on 29 May 2007 are shown in Figure 4. THEMIS B spent a majority of time in the magnetosheath during this event. Although the magnetic field was highly fluctuating, we can conclude that B_z (Figure 4a) was negative at the beginning of the event from 1720 to 1850 UT, but it turned to positive values after 2100 UT, indicating that the IMF B_z sign changed over time in the magnetosheath while the radial IMF was steady (Figure 4e). In agreement with the expectations from the draping

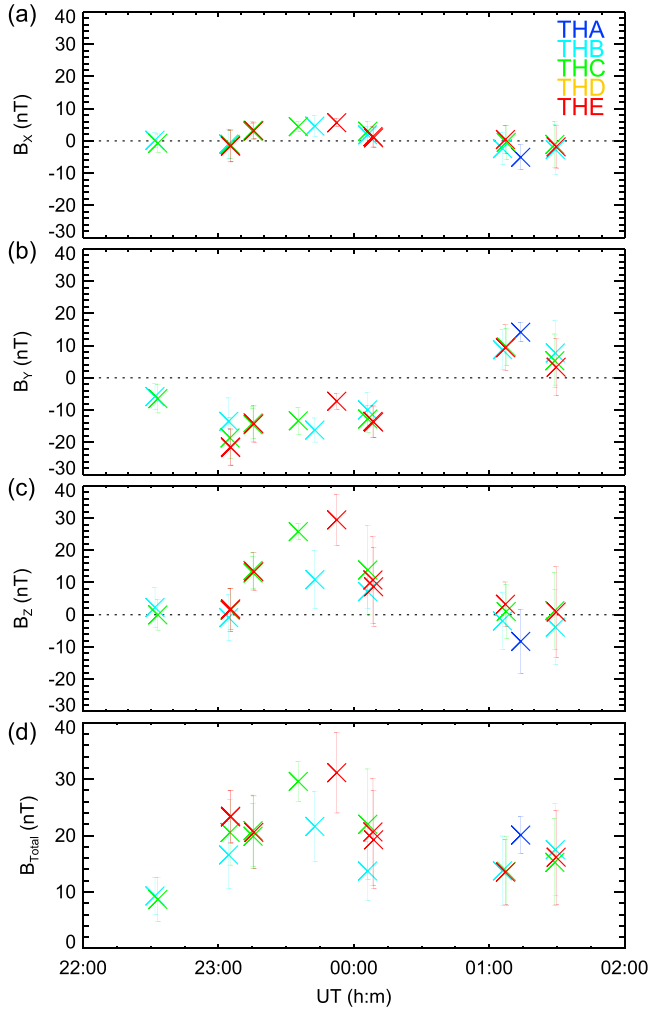

Figure 3. Temporal variations of the magnetosheath magnetic field in the GSM coordinate for the events shown in Figure 2. The different colors correspond to different THEMIS probes. The components (a) B_x, (b) B_y, (c) B_z, and (d) B_{Total} are shown.

effect, B_y or B_z became a principal magnetic field component at the end of the event. The magnetosheath B_x was mostly around zero and did not exhibit any notable change in this period (Figure 4a), similar to the first event. The B_y component started with a value around zero and became positive from 1940 UT to the end of the event (Figure 4a). Due to a similar trajectory (Figure 1b), other THEMIS probes observed similar magnetic field changes. Figure 5a shows the plot of the average magnetosheath B_x in the vicinity of the magnetopause for 29 May 2007. The magnetosheath B_x behavior is similar to the first event with small and around zero fluctuating values, except one point around −10 nT. The magnetosheath B_y profile differs from the first event (Figure 5b). In spite of the spacecraft location and expected draping effect, the value of B_y was mostly smaller than 5 nT except for the THEMIS C period around 2015 UT. The magnetosheath B_z near the magnetopause started with a weak northward orientation (from 0 to 5 nT) around 1830 UT, rotated into a weak southward direction, came back to northward again after 2000 UT, and stayed positive until the end of the event. Between 2000 UT and 2110 UT, the strength of the northward component was increasing, with a slight decrease at the end of the interval 2100–2120 UT (Figure 5c).

4. Discussion

We studied the evolution of the magnetosheath magnetic field near the magnetopause during the radial IMF conditions. The two cases show that the magnetosheath B_z started with the orientation consistent with the IMF draping around the magnetopause, but it changed its orientation from negative to positive and exhibited an increasing trend although the corresponding IMF is stable. Figure 6a shows an illustration of the magnetic field configuration near the magnetopause in the noon meridian plane. When IMF B_x is dominating, the magnetic field direction follows the flow and the draping effect converts it into the B_z and B_y components [*Pi et al.*, 2016]. A confirmation of such magnetic field configuration can also be found in the simulation results by *Tang et al.* [2013]. When IMF B_x points earthward, the magnetic field near the magnetopause points southward in the Southern Hemisphere, but it points northward in the Northern Hemisphere as illustrated in Figure 6a. On the contrary, a sunward radial IMF turns to a negative B_z in the Northern Hemisphere and to a positive B_z in the Southern Hemisphere. In the events under consideration, the THEMIS probes were located in the Southern Hemisphere near the equatorial plane. According to the configuration of the draped field lines with opposite signs of B_z above and below the equator shown in

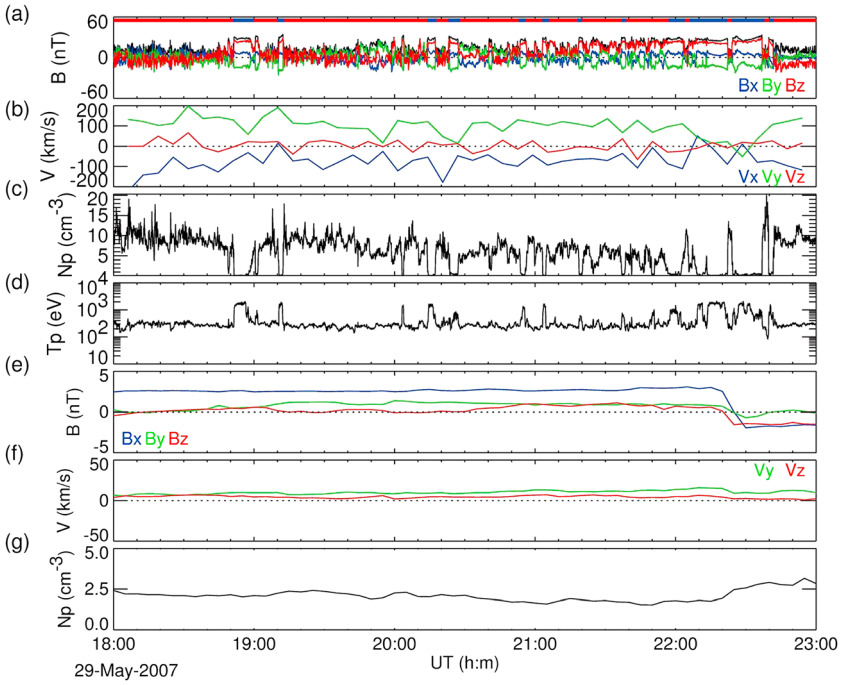

Figure 4. The magnetic field and plasma data changes over time on 29 May 2007. The three components of the (a) magnetic field, (b) plasma speed in the GSM coordinate, (c) proton number density, and (d) proton temperature are arranged. These parameters were obtained from THEMIS B. The simultaneous observations of the (e) magnetic field, (f) solar wind speed, and (g) proton density from the OMNI database. The horizontal bars denote that the probe location is in the magnetosheath (red) and in the magnetosphere (blue).

Figure 6a, the THEMIS probes should observe negative B_z in the 12 July 2007 event with earthward IMF and positive B_z in the 29 May 2007 event with sunward IMF, but our two-case study shows some conflict with these expectations as discussed in the previous section.

4.1. Influence of the Upstream IMF

In addition to the draping effect, the magnetic field structure would follow the changes of the upstream IMF. The propagation time of the observation at the L1 point to the nose of the bow shock is hard to be determined under the radial IMF conditions [*Suvorova and Dmitriev*, 2015b]. Therefore, we cannot compare the OMNI data with the THEMIS data point by point, but the IMF variations are similar to the magnetic field behavior observed near the magnetopause. During the first event, IMF B_z started with a value around zero from 2200 to 2340 UT (see Figure 2e). From 2340 to 0040 UT, IMF B_z was positive. At the end of the event, IMF B_z varied from positive to negative during the interval 0100–0145 UT. We note that mostly negative B_z component was observed in the magnetosheath at the same time. The relation between downstream and upstream magnetic field was also found in the B_y component. IMF B_y was mostly negative from 2200 to 0020 UT. From 0020 UT until the end of the first event, B_y was positive. From 2200 UT to 0030 UT, B_y near the magnetopause was negative and changed to positive after 0030 UT. These observations show a good correlation between the orientation of the IMF B_y and the B_y components in the magnetosheath. In the event of 29 May 2007 (Figure 4e), IMF B_z started with the value around zero and became positive after 2032 UT, similar to the magnetosheath B_z component behavior. B_x was always around zero in the region near the magnetopause; thus, we cannot find the relationship between IMF B_x and the B_x component near the magnetopause in both of the events.

The above comparison reveals that the magnetosheath magnetic field *Y* and *Z* components approximately follow the trends of the corresponding IMF components. Nevertheless, it is hard to quantitatively explain the huge enhancements of B_z. Based on the Rankine-Hugoniot jump conditions, the magnetic field strength can be enhanced up to 4 times with respect to its upstream value in the region near the bow shock [*Viñas and Scudder*, 1986]. However, only the magnetic field components perpendicular to the shock normal can be

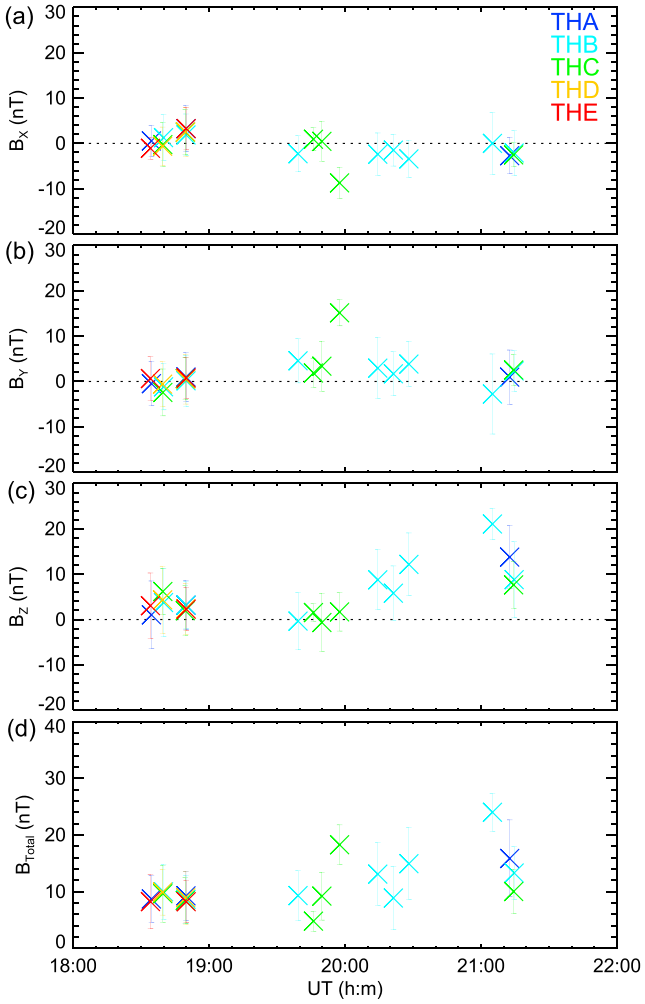

Figure 5. Temporal variations of the magnetosheath magnetic field in the GSM coordinate for the events shown in Figure 4. The different colors correspond to different THEMIS probes. The components (a) B_x, (b) B_y, (c) B_z, and (d) $B_{\text{Total }z}$ components are shown.

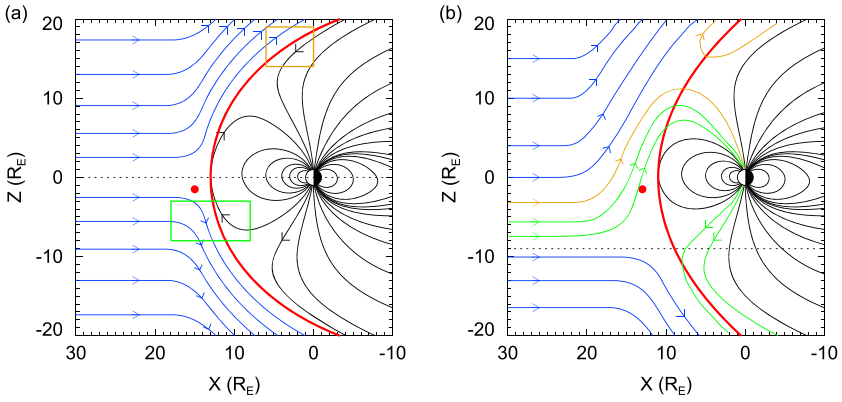

Figure 6. An illustration of the magnetic field structures changing over time near the magnetopause for earthward IMF B_x. There are (a) the initial configuration and (b) the configuration after magnetic reconnection. The green and yellow boxes in Figure 6a indicate the locations where the antiparallel magnetic fields are found. In Figure 6b, the green and yellow lines denote new open field lines created due to the magnetic reconnection. In Figures 6a and 6b, the red points mark the locations of the THEMIS probes at the time of the observations.

enhanced. Since the direction of the bow shock normal near the nose of the bow shock is close to the *X* direction, B_x would conserve its value, but the tangential components (B_y and B_z) would be enhanced. However, our observations made far away from the bow shock show that the enhancement ratio can be much larger than 4. In the magnetosheath, some processes such as the field draping, slow mode structure [*Song et al*., 1992], and the depletion layer [*Midgley and Davis*, 1963] may also change the magnetic field structure. *Pi et al*. [2016] showed an example of the B_x component conversion into B_y and B_z in the magnetosheath. They reported that the maximum difference between IMF and the magnetosheath B_y is around 8 times, including the enhancement through the crossing of the bow shock and the conversion from B_x. The slow mode structure is defined as a region with an increasing density and a decreasing magnetic field due to the slow mode in front of the magnetopause. Some of the crossings identified in this study show the increasing density and a decreasing magnetic field in front of the magnetopause, for instance, the crossing around 00:10 on 12 July 2007. On the contrary, the depletion layers are usually formed due to the compressed magnetic field in front of the magnetopause when the plasma moves away along the field lines. The increasing magnetic field and decreasing density layer cannot be clearly identified in our crossings, which might be related to the quasi-parallel subsolar bow shock under the radial IMF conditions. The depletion layer is usually formed due to the compressed magnetic field in front of the magnetopause when the magnetic field lines are about perpendicular to the magnetopause normal and are piled up near the subsolar point. However, if the magnetic field lines are parallel or quasi-parallel with the magnetopause normal, as in the case of radial IMF, the field lines will be draping around the magnetopause rather than pilling up in front of the magnetopause.

Considering changes in the B_y component in our study, the maximum absolute value of IMF B_y was 1.23 nT for the event on 12 July 2007 and 1.37 nT for the event on 29 May 2007. In the first event (Figure 3b), the magnitude of the magnetosheath B_y was 5–20 nT, regardless of its polarity. The amplification factor of IMF B_y ranges from 5 to 16. In the second event (Figure 5b), the magnitude of the magnetosheath B_y was usually lower than 5 nT, except the extreme value around 1958 UT, and the ratio of the IMF B_y and the magnetosheath B_y does not exceed 5. When the magnetic field approaches the magnetopause, the draping and compression effects will increase the difference between the IMF and the magnetic field in the magnetosheath. *Pulinets et al*. [2012] showed that B_y in front of the magnetopause can be enhanced around 6 to 7 times in comparison with the corresponding IMF B_y. Considering all the processes that enhance the magnetic field in the magnetosheath, ratio of 5–16 of the IMF B_y component and the magnetosheath B_y component is reasonable; however, the B_z enhancement in the magnetosheath can be even larger than B_y enhancement in our study. The maximum value of IMF B_z is 1.01 nT (1.11 nT) for the event on 12 July 2007 (29 May 2007). In Figure 3c, we can find the maximum value of the magnetosheath B_z larger than 20 nT, even approaching 30 nT. The maximum changes of the field components from the solar wind to the magnetosheath were from 1.23 to 21.64 nT for B_y and from 1.01 to 29.43 nT for B_z. In the second event, enhancements are from 1.37 to 15.14 nT for B_y and 1.11 to 21.07 nT for B_z. One can see that enhancement rate of B_z is larger than that for B_y. It implies that the field lines are compressed in the *Z* direction more than in the *Y* direction, or there are other mechanisms that enhance the magnitude of the magnetic field in the *Z* direction.

4.2. Possible Role of Reconnection

Reconnection between the magnetosheath and magnetospheric magnetic field lines is one possible mechanism that changes the magnetic field structure in the magnetosheath near the magnetopause. Figure 6 presents a scenario of the magnetic field evolution under an earthward IMF orientation. With the asymmetric magnetic orientation in the magnetosheath, dayside reconnection happens most likely in the Southern Hemisphere, where the magnetic fields are antiparallel, as shown in the green box in Figure 6a. If reconnection takes place, the closed magnetospheric field line is broken into two open field lines (the green lines in Figure 6b). One of them will move southward and take the magnetic flux to the magnetotail, but the other one would move northward and will be stopped by the magnetic field lines in the dayside magnetosheath (see the green lines in Figure 6b). Therefore, the magnetic flux will be piled up near the subsolar point. The dashed lines in Figure 6 denote the plane that separates northward and southward magnetic fields in the magnetosheath. This plane is shifted to the Southern Hemisphere after reconnection. If reconnection proceeds, the central plane will shift southward even farther. The figure illustrates a situation for earthward IMF B_x; a sunward B_x would result in a northward shift of the plane that divides positive and negative B_z

outside the magnetopause. It should be noted that dayside reconnection would lead to an enlargement of the region near the magnetopause affected by the positive B_z component in the magnetosheath regardless of the IMF B_x sign. This simple scenario can describe the gradual increase of the magnetic field B_z component shown in Figures 3c and 5c. As shown in Figures 3d and 5d, B_{Total} has the same trend as B_z for both events. The enhancement of B_{Total} in the magnetosheath provides the evidence that the pileup process was ongoing for at least part of the time.

At the beginning of the 12 July 2007 case, the THEMIS probes stayed at the Southern Hemisphere (see the red dot in Figure 6). The probes observed the magnetic field with a value close to zero or weakly southward because of the draped field in the magnetosheath near the magnetopause. In the suggested scenario, reconnection would shift the plane that separates two magnetic field with different orientation of the B_z component in the magnetosheath (the dotted lines in Figure 6), and the magnetic field at the observed location would rotate into the northward direction and increase further over time until 0100 UT. Providing the steady IMF orientation, the process described above can last for several hours, as we can see in Figure 3c from 2230 to 0030 UT or in Figure 5c from 1930 to 2130 UT. The magnetosheath B_z can reach values in excess of +20 nT.

Another site where draped IMF and magnetospheric field lines are antiparallel is behind the northern cusp, as it is shown in the yellow box in Figure 6a. The reconnection rate at this place is usually low because the magnetosheath speed is often super-Alfvénic, but the magnetic field pileup increases the Alfvén speed just at the magnetopause. If reconnection happens behind the northern cusp, one of the new field lines will be brought by the flow to the magnetotail and the other one will also pile up at the dayside (see the yellow lines in Figure 6b).

Suggested scenario cannot explain the abrupt change of the magnetosheath B_z from the largely positive to around zero after 0030 UT, as shown in Figure 3c in the first event. However, this change may be related to the variation of the upstream solar wind parameters. Figure 2f shows the solar wind V_y and V_z components from the OMNI data set. It can be seen from the figure that the V_y changes from positive into negative at 0000 UT. Variations in the east-west component of the solar wind velocity will cause the changes in the draping of magnetic field lines around the magnetopause. In the second event on 29 May 2007, the upstream solar wind velocity did not exhibit any similar changes and we did not observe any strong decrease of the B_z component at the end of the interval.

Suggested scenario of two possible reconnection locations also can explain the observations during the second event. The THEMIS probes were located in the Southern Hemisphere,but near the geomagnetic equator at about 15 MLT, and the magnetic field B_z component in the magnetosheath was small and positive at the beginning of the analyzed interval. This orientation is consistent with the sunward IMF and the expected initial IMF draping. A decrease of the B_z component, even to slightly negative values at ~1945 UT, can be connected with foreshock fluctuations that modulate the IMF direction, but the following increase of this component to 15–20 nT is fully compatible with the suggested scenario. This scenario shows that the magnetic field near the equatorial magnetopause would point increasingly northward as the dayside and/or northern lobe reconnection proceeds. Dayside reconnection is also noticeable from the MHD simulations of *Tang et al*. [2013]. Moreover, *Tang et al*. [2013] also predicted the reconnection site behind the northern cusp for negative IMF B_x.

Variations in the magnetosheath magnetic field strength and orientation can also be possibly explained by the position of the observation, i.e., changes of the THEMIS location in time. In Figure 1b, we can see that THEMIS B moved northward around 2 R_E during the period under study in the second case. It means that the probe is moving to the southward magnetic field-dominated region according to the expected draping effect for radial IMF conditions. It is one of the reasons that the enhancement of B_z near the magnetopause is smaller than in the first case, as the motion of the probes during the second event can cause a decreasing in the B_z component during 1830–1945 UT.

The observational evidence for suggested reconnection scenarios is only indirect, but the THEMIS probes observed the variation in the boundary layer thickness that probably comes from the reconnection. Previous studies [*Song and Russell*, 1992; *Song et al*., 1999, *Němeček et al*., 2015] suggested that the low-latitude boundary layer (LLBL) is formed by reconnection poleward of cusps in one or both hemispheres under the northward IMF condition. Lobe reconnection at one hemisphere creates the

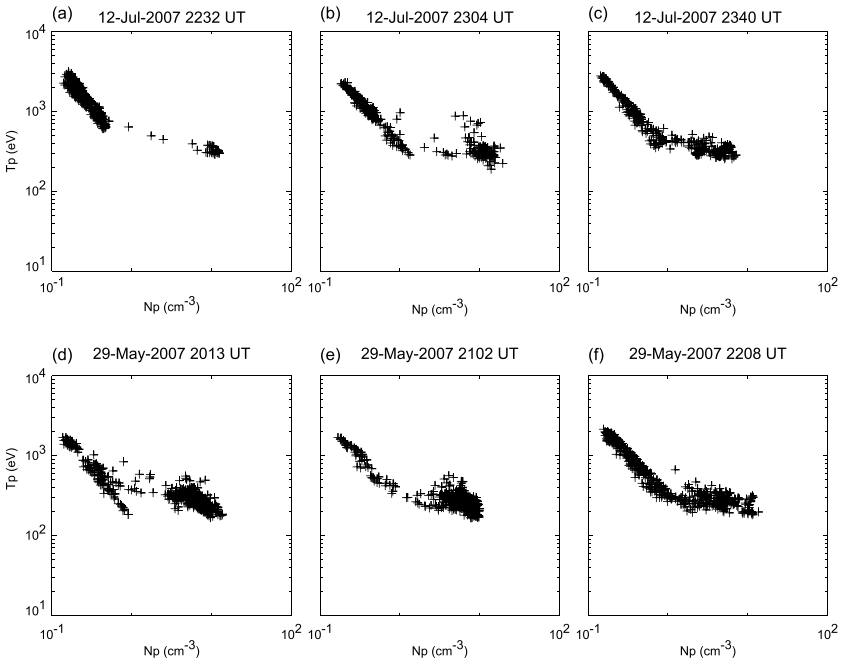

Figure 7. The *n-T* plots changed over time in the two events. (a–c) The *n-T* plots in different times for the event on 12 July 2007 and (d–f) the *n-T* plots for the event on 29 May 2007.

LLBL on open field lines. If the magnetosheath B_z is large enough, the same magnetic field line can reconnect again in the conjugated hemisphere and increase the thickness of the LLBL on the closed field lines. Closed field lines are usually located inside the magnetopause, but the open field lines extend through the magnetosheath into the solar wind. This scenario is generally accepted, but different authors use different names for particular parts of the magnetosheath-magnetosphere interface. For example, *Hasegawa* [2012] divide the interface into three sublayers—the inner LLBL on closed field lines and outer LLBL and magnetosheath boundary layer (MSBL) on open field lines. On the other hand, *Le et al.* [1996] argued that single lobe reconnection forms the outer LLBL, whereas the inner LLBL is on closed field lines. It means that the MSBL of *Hasegawa* [2012] and the outer LLBL of *Le et al.* [1996] are on the same field lines, but the name MSBL emphasizes an extension of the field lines to the magnetosheath, whereas the LLBL suggests that it is a part of the magnetosphere. These classifications are based on the magnetic field topology that can be easily determined in the computer model because each field line can be easily traced. On the other hand, a decision whether the spacecraft in a particular time and place is on open or closed field lines is more difficult. Pitch angle distributions of electrons and/or ions are usually used for this purpose—bidirectional population (parallel and antiparallel) and electron population with the balanced fluxes at all energies would be a signature of closed field lines [*Bogdanova et al.*, 2008], whereas particles streaming from the reconnection site would be found on open field lines. However, an exact distinction between these two possibilities requires measurements of full 3-D particle distributions with sufficient time resolution [e.g., *Øieroset et al.*, 2015], which are not available in our events. In this study, the main purpose is to investigate the magnetic field structure outside the magnetopause; therefore, the separation of boundary layer is not a concern here. In Figure 6b, the configuration is similar to single lobe reconnection under the northward IMF condition but there is no possibility of the lobe reconnection in the Southern Hemisphere due to asymmetric magnetic field orientation in the magnetosheath and, therefore, no possibility of dual lobe reconnection. Once reconnection at the dayside magnetopause or poleward of the cusp takes place, it can form the LLBL and MSBL, as the yellow and green lines in Figure 6 indicate.

Figure 7 shows the *n-T* plots for two events. The *n-T* plot is a powerful tool to judge each layer near the magnetopause [*Hapgood and Bryant*, 1992; *Němeček et al.*, 2015]. As density and temperature have different values inside each layer (magnetosphere, LLBL, MSBL, and magnetosheath), they will be distributed in

different locations in the *n-T* plot. In Figure 7, the ion density and temperature data with the 3 s resolution are used. The high temperature (usually higher than 10^3 eV) and low density (lower than few cm^{-3}, as in the left upper part in Figure 7a) are characteristics of the plasma in the magnetosphere, whereas the low temperature (around 10^2–10^3 eV) and high density (higher than 5 cm^{-3}, as in the right middle part in the Figure 7a) are signatures of the magnetosheath region. Figures 7a–7c present the *n-T* plots for three different magnetopause crossings during the interval 2232–2340 UT in the first event. In Figure 7a, a clear gap between the magnetosphere and magnetosheath particles can be seen. In Figure 7b, some particles appear between these two regions and the gap disappears in Figure 7c. This sequence reveals that the boundary layer is formed gradually during the period when the magnetic field outside the magnetopause turns northward (Figure 3c). Figures 7d–7f show the *n-T* plots from 2013 to 2208 UT on 29 May 2007, and a similar behavior of plasma parameters can be also found in this event. At 2013 UT (Figure 7d), the presence of the boundary layer is unclear. More particles appeared in the boundary layer at 2102 UT (Figure 7e), and the structure in the *n-T* plot became continuous in Figure 7f that corresponds to the time when the magnetic field outside the magnetopause was northward.

Missing observations of the boundary layer can be caused by the fast magnetopause motion. To understand if the observed variations of the LLBL structure are connected with the magnetopause motion, we estimated the speed of the magnetopause using locations of probes and the times of multiple crossings. We used all pairs of crossings that THEMIS probes observed in order to estimate the magnetopause speed under assumption that the magnetopause normal is in the *X* direction near the Sun-Earth line. For three selected magnetopause crossings on 12 July 2007, at 2230–2232, 2303–2304, and 2340–2344 UT (Figures 7a–7c), the speeds of the magnetopause motion were 21.2, 1.2, and 7.88 km/s, respectively. The magnetopause was moving quickly at 2232 UT, and just a few data points in the boundary layer were observed. For this crossing, we cannot exclude the influence of the fast magnetopause motion. Nevertheless, the magnetopause motion during the last two crossings, especially during the crossing observed at 2304 UT, was slower than that during the first crossing. The LLBL/MSBL structure was not clear during first two crossings, but this structure was fully developed during the crossing at 2340 UT with a relatively high speed. Therefore, the LLBL/MSBL structure variations through the period from 2304 to 2340 UT (Figures 7b and 7c) cannot be explained by the influence of the fast magnetopause motion on a determination of the boundary structure. In addition, we cannot assume the normal of the magnetopause in the second event. Therefore, the speeds of the magnetopause in the second event have not been calculated in this study.

5. Conclusions

The THEMIS probes crossed the magnetopause on 12 July 2007 and 29 May 2007 under the radial IMF, but these two events exhibit opposite IMF B_x polarities. In our two-case study, B_z in the magnetosheath started with the opposite polarities, but it turned northward with an increasing trend near the magnetopause. This phenomenon can be attributed to two mechanisms: changes of the upstream IMF and reconnection that occurs between the magnetosheath and the magnetospheric magnetic field lines. The draping effect forms a north-south asymmetry of the B_z orientation at the beginning of the event. Both cases exhibit similar changes of the IMF B_z component in the magnetosheath near the magnetopause: at the beginning of the intervals B_z is very small and it rotates northward as the time proceeds. These IMF B_z variations may cause the positive turn of the magnetosheath B_z and its enhancement, but the enhancement rate is much larger than the changes of IMF B_z. Asymmetric reconnection under the radial IMF is the other possible mechanism to change the magnetosheath B_z orientation and strength near the magnetopause. The antiparallel orientation of the magnetosheath and magnetospheric magnetic fields can cause reconnection at the dayside magnetopause at different locations for the different B_x polarities. Under a sunward radial IMF, reconnection may occur at the dayside magnetopause in the Northern Hemisphere and behind the cusp in the Southern Hemisphere. For an earthward IMF, the reconnection sites will be reversed. Reconnection at different hemispheres forms new open field lines and reconfigures the magnetic field structure in the magnetosheath. It would shift the central plane of the asymmetric structure of the magnetic field direction in the magnetosheath. A plane dividing northward and southward pointing magnetosheath magnetic fields at the magnetopause would shift northward of the geomagnetic equator for the sunward pointing IMF and southward for the earthward

pointing IMF. Both shifts cause the enhancement of positive B_z in the magnetosheath near the subsolar magnetopause. This reconnection scenario can explain observed variations of the magnetic field in the magnetosheath near the magnetopause, but unfortunately, the time resolution of the available plasma data is not sufficient to undoubtedly confirm it.

Acknowledgments
This work was supported by grants NSC-102-2923-M-008-003 and NSC-104-2111-M-008-018 to the National Central University and by the grant 17-60605S to the Czech Science Foundation. We thank Joe King and Natalia Papitashvili of the National Space Science Data Center (NSSDC) in the NASA/GSFC for the use of the OMNI 2 database and V. Angelopoulos for the use of data from THEMIS mission. The OMNI data were provided by the Space Physics Data Facility (SPDF) in the NASA/GSFC, http://omniweb.gsfc.nasa.gov/. The THEMIS data were obtained from the coordinated data analysis web (CDAWeb), http://cdaweb.gsfc.nasa.gov/cdaweb.

References

Auster, H. U., et al. (2008), The Themis mission, *Space Sci. Rev.*, *141*, 5–34, doi:10.1007/s11214-008-9336-1.

Bogdanova, Y. V., et al. (2008), Formation of the low-latitude boundary layer and cusp under the northward IMF: Simultaneous observations by Cluster and Double Star, *J. Geophys. Res.*, *113*, A07S07, doi:10.1029/2007JA012762.

Bogdanova, Y. V., C. J. Owen, M. W. Dunlop, M. G. G. T. Taylor, and A. N. Fazakerley (2013), Magnetospheric boundary layer structure and dynamics as seen from cluster and double star measurements, *Chin. J. Space Sci.*, *33*(6), 577–603, doi:10.11728/cjss2013.06.577.

Chao, J. K., D. J. Wu, H.-H. Lin, Y.-H. Ynag, M. Kessel, S. H. Chen, and R. P. Lepping (2002), Models for the size and shape of the Earth's magnetopause and bow shock, *COSPAR Colloq. Ser.*, *12*(C), 127–135, doi:10.1016/S0964-2749(02)80212-8.

Crooker, N. . U. (1979), Dayside merging and cusp geometry, *J. Geophys. Res.*, *84*, 951–959, doi:10.1029/JA084iA03p00951.

Dungey, J. W. (1961), Interplanetary magnetic field and the auroral zone, *Phys. Rev. Lett.*, *6*, 47–48, doi:10.1103/PhysPevLett.6.47.

Dungey, J. W. (1963), The structure of the ionosphere, or adventures in velocity space, in *Geophysics: The Earth's Environment*, edited by C. Dewitt, J. Hieblot, and A. Lebeau, pp. 503–550, Gordon and Breach, New York.

Dušík, S., G. Granko, J. Šafránková, Z. Němeček, and K. Jelínek (2010), IMF cone angle control of the magnetopause location: Statistical study, *Geophys. Res. Lett.*, *37*, L19103, doi:10.1029/2010GL044965.

Hapgood, M. . A., and D. A. Bryant (1992), Exploring the magnetospheric boundary layer, *Planet. Space Sci.*, *40*, 1431–1459, doi:10.1016/0032-0633(92)90099-A.

Hasegawa, H. (2012), Structure and dynamics of the magnetopause and its boundary layers, *Monogr. Environ. Earth Planets*, *1*, 71–119, doi:10.5047/meep.2012.00102.0071.

Hietala, H., T. V. Laitinen, K. Andréeová, R. Vainio, A. Vaivads, M. Palmroth, T. I. Pulkkinen, H. E. J. Koskinen, E. A. Lucek, and H. Rème (2009), Supermagnetosonic jets behind a collisionless quasiparallel shock, *Phys. Rev. Lett.*, *103*, 245001, doi:10.1103/PhysRevLett.103.245001.

Huang, T., H. Wang, J.-H. Shue, L. Cai, and G. Pi (2015), The dayside magnetopause location during radial interplanetary magnetic field periods: Cluster observation and model comparison, *Ann. Geophys.*, *33*, 437–448, doi:10.5194/angeo-33-437-2015.

Jelínek, K., Z. Němeček, J. Šafránková, J.-H. Shue, A. V. Suvorova, and D. G. Sibeck (2010), Thin magnetosheath as a consequence of the magnetopause deformation: THEMIS observations, *J. Geophys. Res.*, *115*, A10203, doi:10.1029/2010JA015345.

Jones, G. H., A. Balogh, and R. J. Forsyth (1998), Radial heliospheric magnetic fields detected by Ulysses, *Geophys. Res. Lett.*, *25*(16), 3109–3112, doi:10.1029/98GL52259.

King, J. H., and N. E. Papitashvili (2005), Solar wind spatial scales in and comparisons of hourly Wind and ACE plasma and magnetic field data, *J. Geophys. Res.*, *110*, A02104, doi:10.1029/2004JA010649.

Le, G., C. T. Russell, J. T. Gosling, and M. F. Thomsen (1996), ISEE observations of low-latitude boundary layer for northward interplanetary magnetic field: Implications for cusp reconnection, *J. Geophys. Res.*, *101*, 239–249, doi:10.1029/96JA02528.

McFadden, J. P., C. W. Carlson, D. Larson, J. Bonnell, F. S. Mozer, V. Angelopoulos, K.-H. Glassmeier, and U. Auster (2008), THEMIS ESA plasma instrument and in-flight calibration, *Space Sci. Rev.*, *141*, 277–302, doi:10.1007/s11214-008-9440-2.

Midgley, J. E., and L. Davis Jr. (1963), Calculation by a moment technique of the perturbation of the geomagnetic field by the solar wind, *J. Geophys. Res.*, *68*(18), 5111–5123, doi:10.1029/JZ068i018p05111.

Němeček, Z., J. Šafránková, O. Kruparova, L. Přech, K. Jelínek, Š. Dušík, J. Šimůnek, K. Grygorov, and J.-H. Shue (2015), Analysis of temperature versus density plots and their relation to the LLBL formation under southward and northward IMF orientations, *J. Geophys. Res. Space Physics*, *120*, 3475–3488, doi:10.1002/2014JA020308.

Neugebauer, M., R. Goldstein, and B. E. Goldstein (1997), Features observed in the trailing regions of interplanetary clouds from coronal mass ejections, *J. Geophys. Res.*, *102*(A9), 19,743–19,751, doi:10.1029/97JA01651.

Øieroset, M., T. D. Phan, J. T. Gosling, M. Fujimoto, and V. Angelopoulos (2015), Electron and ion edges and the associated magnetic topology of the reconnecting magnetopause, *J. Geophys. Res. Space Physics*, *120*, 9294–9306, doi:10.1002/2015JA021580.

Omidi, N., J. P. Eastwood, and D. G. Sibeck (2010), Foreshock bubbles and their global magnetospheric impacts, *J. Geophys. Res.*, *115*, A06204, doi:10.1029/2009JA014828.

Park, J.-S., J.-H. Shue, K.-H. Kim, G. Pi, Z. Němeček, and J. Šafránková (2016), Global expansion of the dayside magnetopause for long-duration radial IMF events: Statistical study on GOES observations, *J. Geophys. Res. Space Physics*, *121*, 6480–6492, doi:10.1002/2016JA022772.

Parker, E. N. (1958), Dynamics of the interplanetary gas and magnetic fields, *Astrophys. J.*, *128*, 664, doi:10.1086/146579.

Petrinec, S. M. (2016), Draping of strongly flow-aligned interplanetary magnetic field about the magnetopause, *Adv. Space Res.*, *58*(2), 175–180, doi:10.1016/j.asr.2015.10.001.

Pi, G., J.-H. Shue, J.-K. Chao, Z. Němeček, J. Šafránková, and C.-H. Lin (2014), A reexamination of long-duration radial IMF events, *J. Geophys. Res. Space Physics*, *119*, 7005–7011, doi:10.1002/2014JA019993.

Pi, G., J.-H. Shue, J.-S. Park, J.-K. Chao, Y.-H. Yang, and C.-H. Lin (2016), A comparison of the IMF structure and the magnetic field in the magnetosheath under the radial IMF conditions, *Adv. Space Res.*, *58*(2), 181–187, doi:10.1016/j.asr.2015.11.012.

Pulinets, M. S., M. O. Ryazantsev, E. E. Antonova, and I. P. Kirpichev (2012), Dependence of magnetic field parameters at the subsolar point of the magnetosphere on the interplanetary magnetic field according to the data of the THEMIS experiment, *Geomagn. Aeron.*, *52*, 730, doi:10.1134/S0016793212060084.

Russell, C. T., S. M. Petrinec, T. L. Zhang, P. Song, and H. Kawano (1997), The effect of foreshock on the motion of the dayside magnetopause, *Geophys. Res. Lett.*, *24*(12), 1439–1441, doi:10.1029/97GL01408.

Samsonov, A. A., Z. Nemecek, J. Safrankova, and K. Jelinek (2012), Why does the subsolar magnetiopause move sunward for radial interplanetary magnetic field?, *J. Geophys. Res.*, *177*, A05221, doi:10.1029/2011JA017429.

Shue, J.-H., J. K. Chao, H. C. Fu, C. T. Russell, P. Song, K. K. Khurana, and H. J. Singer (1997), A new functional form to study the solar wind control of the magnetopause size and shape, *J. Geophys. Res.*, *102*(A5), 9497–9511, doi:10.1029/97JA00196.

Shue, J.-H., J.-K. Chao, P. Song, J. . P. McFadden, A. Suvorova, V. Angelopoulos, K. . H. Glassmeier, and F. Plaschke (2009), Anomalous magnetosheath flows and distorted subsolar magnetopause for radial interplanetary magnetic fields, *Geophys. Res. Lett.*, *36*, L18112, doi:10.1029/2009GL039842.

Shue, J.-H., et al. (2011), Uneven compression levels of Earth's magnetic fields by shocked solar wind, *J. Geophys. Res.*, *116*, A02203, doi:10.1029/2010JA016149.

Sibeck, D. G., and V. Angelopoulos (2008), THEMIS science objectives and mission phases, *Space Sci. Rev.*, *141*, 35–59, doi:10.1007/s11214-008-9393-5.

Slavin, J. A., A. Szabo, M. Peredo, R. P. Lepping, R. J. Fitzenreiter, K. W. Ogilvie, C. J. Owen, and J. T. Steinberg (1996), Near-simultaneous bow shock crossings by WIND and IMP 8 on December 1, 1994, *Geophys. Res. Lett.*, *23*(10), 1207–1210, doi:10.1029/96GL01351.

Song, P., and C. T. Russell (1992), Model of the formation of the low-latitude boundary layer for strongly northward interplanetary magnetic field, *J. Geophys. Res.*, *97*(A2), 1411–1420, doi:10.1029/91JA02377.

Song, P., C. T. Russell, and M. F. Thomsen (1992), Slow mode transition in the frontside magnetosheath, *J. Geophys. Res.*, *97*(A6), 8295–8305, doi:10.1029/92JA00381.

Song, P., D. L. DeZeeuw, T. I. Gombosi, C. P. T. Groth, and K. G. Powell (1999), A numerical study of solar wind-magnetosphere interaction for northward interplanetary magnetic field, *J. Geophys. Res.*, *104*(A12), 28,361–28,378, doi:10.1029/1999JA900378.

Sundkvist, D., A. Retino, A. Vaivads, and S. D. Bale (2007), Dissipation in turbulent plasma due to reconnection in thin current sheets, *Phys. Rev. Lett.*, *99*(2, 025004), doi:10.1103/PhsRevLett.9.025004.

Suvorova, A. V., and A. V. Dmitriev (2015a), Magnetopause inflation under radial IMF: Comparison of models, *Earth Space Sci.*, *2*, doi:10.1002/2014EA000084.

Suvorova, A. V., and A. V. Dmitriev (2015b), On magnetopause inflation under radial IMF, *Adv. Space Res.*, *58*(12), 29–256, doi:10.1016/j.asr.2015.07.044.

Suvorova, A. V., J.-H. Shue, A. V. Demitriev, D. G. Sibeck, J. P. McFadden, H. Hasegawa, K. Ackerson, K. Jelínek, J. Šafránková, and Z. Němeček (2010), Magnetopause expansions for quasi-radial interplanetary magnetic field: THEMIS and Geotail observation, *J. Geophys. Res.*, *115*, A10216, doi:10.1029/2010JA015404.

Tang, B. B., C. Wang, and W. Y. Li (2013), The magnetosphere under the radial interplanetary magnetic field: A numerical study, *J. Geophys. Res. Space Physics*, *118*, 7674–7682, doi:10.1002/2013JA019155.

Viñas, A. F., and J. D. Scudder (1986), Fast and optimal solution to the "Rankine-Hugoniot problem", *J. Geophys. Res.*, *91*(A1), 39–58, doi:10.1029/JA091iA01p00039.

Watari, S., M. Vandas, and T. Watanabe (2005), Solar cycle variation of long-duration radial interplanetary magnetic field events at 1 AU, *J. Geophys. Res.*, *110*, A12102, doi:10.1029/2005JA011165.